Monthly Notices of the ROYAL ASTRONOMICAL SOCIETY

MNRAS **523,** 5207–5219 (2023) https://doi.org/10.1093/mnras/stad1775
Advance Access publication 2023 June 16

Distinct polarization properties for two emission states of four pulsars

Yi Yan,[1,2] P. F. Wang[1,2]★ and J. L. Han[1,2,3]★

[1]*National Astronomical Observatories, Chinese Academy of Sciences, Beijing 100101, China*
[2]*School of Astronomy, University of Chinese Academy of Sciences, Beijing 100049, China*
[3]*CAS Key Laboratory of FAST, NAOC, Chinese Academy of Sciences, Beijing 100101, China*

Accepted 2023 June 6. Received 2023 June 2; in original form 2023 March 30

ABSTRACT

Four pulsars, PSRs J1838+1523, J1901+0510, J1909+0007, and J1929+1844, are found to exhibit bright and weak emission states from sensitive observations made using the Five-hundred-meter Aperture Spherical radio Telescope (FAST). New FAST observations have measured the polarization properties for the two states, and reveal that the polarization profiles, linear polarization percentage, and polarization position angle curves, as well as circular polarization percentage, are partially or entirely different in the two emission states. Remarkably, PSR J1838+1523 has very different slopes for the polarization position angle curves. PSR J1901+0510 has a wider profile and a higher linear polarization in the weak state than in the bright state. PSR J1909+0007 has very distinct polarization angle curves for the two modes. While in the case of PSR J1929+1844, the central profile component evolves with frequency in the bright state, and the senses of circular polarization are opposite in the two modes. The different polarization properties of the two emission states provide valuable insights into the physical processes and emission conditions in the pulsar magnetosphere.

Key words: pulsars: individual: J1838+1523 – pulsars: individual: J1901+0510 – pulsars: individual: J1909+0007 – pulsars: individual: J1929+1844 – polarization.

1. INTRODUCTION

The mean pulse profile of a pulsar is obtained by averaging hundreds of individual pulses, which is usually stable and represents a unique feature of the pulsar. Soon after its discovery, it was found that the pulse profile of PSR B1237+25 does not always have the same profile, and it sometimes switches to an 'abnormal shape' (Backer 1970). The switching between two or more types of profiles was called 'mode-changing', indicating that the emission modes change for some durations. So far, the mode-changing phenomenon has been observed for dozens of pulsars (e.g. PSRs B0031−07, B1237+25, and J2321+6024; Huguenin, Taylor & Troland 1970; Rahaman et al. 2021; Wang et al. 2022).

In order to get a better understanding of the mode-changing phenomenon, several physical interpretations have been proposed, which are generally related to the different states in the pulsar magnetosphere. For example, Wang, Manchester & Johnston (2007) suggested that redistribution of the magnetospheric current flow results in mode changes or nulling. Different geometries might lead to mode changes (Timokhin 2010). The emission state can also be affected by temporal modifications of the local magnetic field structure and strength at the surface of the polar cap (Geppert et al. 2021). Moreover, changes of pulse profiles were found to be closely related to different spin-down rates of some pulsars (Lyne et al. 2010).

In addition to the change of pulse profiles, the polarization might also be different for the emission of different modes. For instance, different linear polarization degrees of different emission modes have been detected for pulsars such as PSRs J0738−4042, J0742−2822, and J1938+2213 (Karastergiou et al. 2011; Keith, Shannon & Johnston 2013). The circular polarization of the two emission modes might also be different, for example, the opposite senses for PSR B0943+10 (Suleymanova et al. 1998). In some cases, the polarization position angles (PAs) remain consistent between the two emission modes, for pulsars such as PSRs J1822−2256, B0329+54, J2321+6024, and J1727−2739 (e.g. Basu & Mitra 2018; Brinkman, Mitra & Rankin 2019; Rahaman et al. 2021; Rejep et al. 2022). However, the polarization PA curve of PSR J0614+2229 was found to be shifted along the rotation phase for the two emission modes (Sun et al. 2022), which is probably caused by different emission heights for two modes via the aberration effect (Blaskiewicz, Cordes & Wasserman 1991). In some cases (e.g. PSRs J0946+0951, J2006−0807, and J0738−4042), the mode-changing phenomenon is closely related to the orthogonal polarization modes (Suleymanova et al. 1998; Rankin & Suleymanova 2006; Karastergiou et al. 2011; Basu, Paul & Mitra 2019). Ilie et al. (2020) detected the polarization difference of the modulated emission observed for the two drifting modes, and suggested that the change of drifting modes is not only caused by a change in the underlying carousel radius but is also related to magnetospheric propagation effects. Therefore, polarization properties are important keys in probing the physical mechanisms or emission conditions for the mode-changing phenomenon.

During the Galactic Plane Pulsar Snapshot (GPPS) survey (Han et al. 2021) by the Five-hundred-meter Aperture Spherical radio Telescope (FAST; Nan 2006; Nan et al. 2011), areas of the sky with known pulsars have been observed as a verification of the receiver

★ E-mail: pfwang@nao.cas.cn (PFW); hjl@bao.ac.cn (JLH)

Table 1. Parameters of the FAST pulsar observations. Column 1 shows the pulsar name. Columns 2 and 3 give the pulsar period and dispersion measure (DM). Column 4 is the date of observation in the format of yyyy/mm/dd. Column 5 is the cover name and the beam number of the FAST pulsar observations. The symbol * in this column indicates the FAST released archived data for open usage. Column 6 gives the pulsar coordination offset from the beam centre in arcmin. Column 7 is the length of observation time in minute. Column 8 gives the references for mode-changing observations: 0, this paper; 1, Ferguson et al. (1981); 2, Nowakowski (1994); 3, Weisberg et al. (1986).

Name	P0 (s)	DM (cm^{-3} pc)	ObsDate	Cover_Beam	Offset (′)	T_{obs} (min)	Ref.
(1)	(2)	(3)	(4)	(5)	(6)	(7)	(8)
J1838+1523	0.549	67.9	2021/08/08	G45.26+9.83_M09P3	0.80	5	0
J1901+0510	0.615	434.1	2021/05/02	J1901+0510_M01P1*	0.01	27	0
			2021/09/03	J190129+051533_M09P1	1.67	15	
J1909+0007 (B1907+00)	1.017	113.0	2021/07/01	G35.14−3.81_M11P1	0.87	5	0
J1929+1844 (B1926+18)	1.220	112.5	2021/01/11	J1928+1839_M19P1	0.42	30	1, 2, 3
			2022/06/02	J192838+183935_M19P1	0.42	15	

system, and all polarization data have been recorded. Among the large number of pulsars observed, we find four pulsars, PSRs J1838+1523, J1901+0510, J1909+0007, and J1929+1844, exhibiting distinct polarization properties for different emission modes. In this paper, we present the polarization profiles for these mode-changing pulsars. Observations and data processing are briefly presented in Section 2. In Section 3, we report on the results for different emission modes of the four pulsars and we analyse their polarization properties. We present a discussion and conclusions in Sections 4 and 5, respectively.

2. OBSERVATIONS AND DATA REDUCTION

Details of FAST observations of the four pulsars are listed in Table 1. The data of all but one have been taken by the FAST GPPS survey (Han et al. 2021) using the 19-beam *L*-band receivers (Jiang et al. 2020). The other data set is taken from the open data source in the FAST released archive for PSR J1901+0510, which is used here mainly for result verification. The observations cover the frequency range 1000–1500 MHz, with 4096 or 2048 channels. Full polarization signals, *XX*, *YY*, $\Re[X^*Y]$ and $\Im[X^*Y]$, were recorded with a sampling time of 49.152 μs. All pulsars were observed with the zenith angles smaller than 28°.5, so that FAST has a full gain of $G = 16$ K Jy^{-1}. The instrument polarization is calibrated with the solutions obtained from on–off calibration signals around each observation, including the bandpass and polarization response.

Taking pulsar ephemerides from the Australia Telescope National Facility Pulsar Catalogue (Manchester et al. 2005), we de-disperse and fold data using the open source package DSPSR (van Straten & Bailes 2011). PSRCHIVE software (Hotan, van Straten & Manchester 2004) is used to estimate and correct the the Faraday rotation measure .

3. RESULTS AND ANALYSIS

The single-pulse sequence was first plotted for each pulsar, as shown in Figs 1–6. The pulse intensity integrated over the entire pulse window is shown to the right of the sequence. Two distinct emission states or modes are apparent in the pulse sequence, and are further verified in the intensity variations. Some zoomed segments of the pulse sequences and the intensity variations are shown Fig. 7.

The distribution of integrated pulse intensities shown in the subpanel (d) of Figs 1–6 has a bimodal shape. One can therefore set a threshold to distinguish the bright and weak emission states, as indicated by the dashed line in the subpanels (b) and (d). Considering the modulation of pulse intensity by random processes, we ignore a mode lasting for only one or two periods except for the bright pulses of PSR J1901+0510.

The polarized pulse profiles of two discriminated modes are then obtained by integrating single-pulse data, as shown in subpanels in the right parts of Figs 1–6. Their polarization properties are also listed in Table 2.

3.1. PSR J1838+1523

PSR J1838+1523 was found by Surnis et al. (2018) using the Giant Metrewave Radio Telescope (GMRT) at 325 MHz, and a timing solution was published alongside.

This is the first time that the mode changing of PSR J1838+1523 has been reported. The FAST GPPS survey observation of this pulsar was made for only 5 min on 2021 August 8 (hereafter 2021/08/08, as for other observation dates). Its single-pulse sequence exhibits strong emission between pulse numbers 265 and 460, lasting for about 1.8 min, as shown in Fig. 1. The trailing component is significantly enhanced during the bright state, as shown by the normalized intensities in Fig. 1(c).

Moreover, only the trailing component is strengthened during the pulse period of 40–80 in the weak state, which may be another mode, and more, better quality, data are needed to make any conclusions.

The linear polarization intensity and the fractional linear polarization vary over the profile components, and they are different in the two states, as shown in subpanels (e)-(k). The polarization PA curve in the profile trailing parts in the bright state has a steeper slope than that in the weak state. Their ellipticity angles show differences in the longitude range from −15° to −6°. In addition, the strongest trailing component in the bright state seems to have flux modulations (see Fig. 7), indicating plasma activity in the pulsar magnetosphere.

3.2. PSR J1901+0510

PSR J1901+0510 was discovered by the Parkes multibeam pulsar survey (Hobbs et al. 2004).

We obtained a FAST observation for 15 min of PSR J1901+0510 on 2021/09/03 during the confirmation observation of a pulsar candidate through one of the 19 beams. As shown in Fig. 3, the pulse sequence shows that its bright and weak states switch very frequently (see the zoomed-in single-pulse sequence in Fig. 7). The bright state is maintained for only one or a few periods, while the radio emission is very weak for most periods.

To verify such a quick mode-switching, we take archived FAST data observed on 2021/05/02 for 27 min, and the results are shown in Fig. 2. The switching between both emission states is then confirmed,

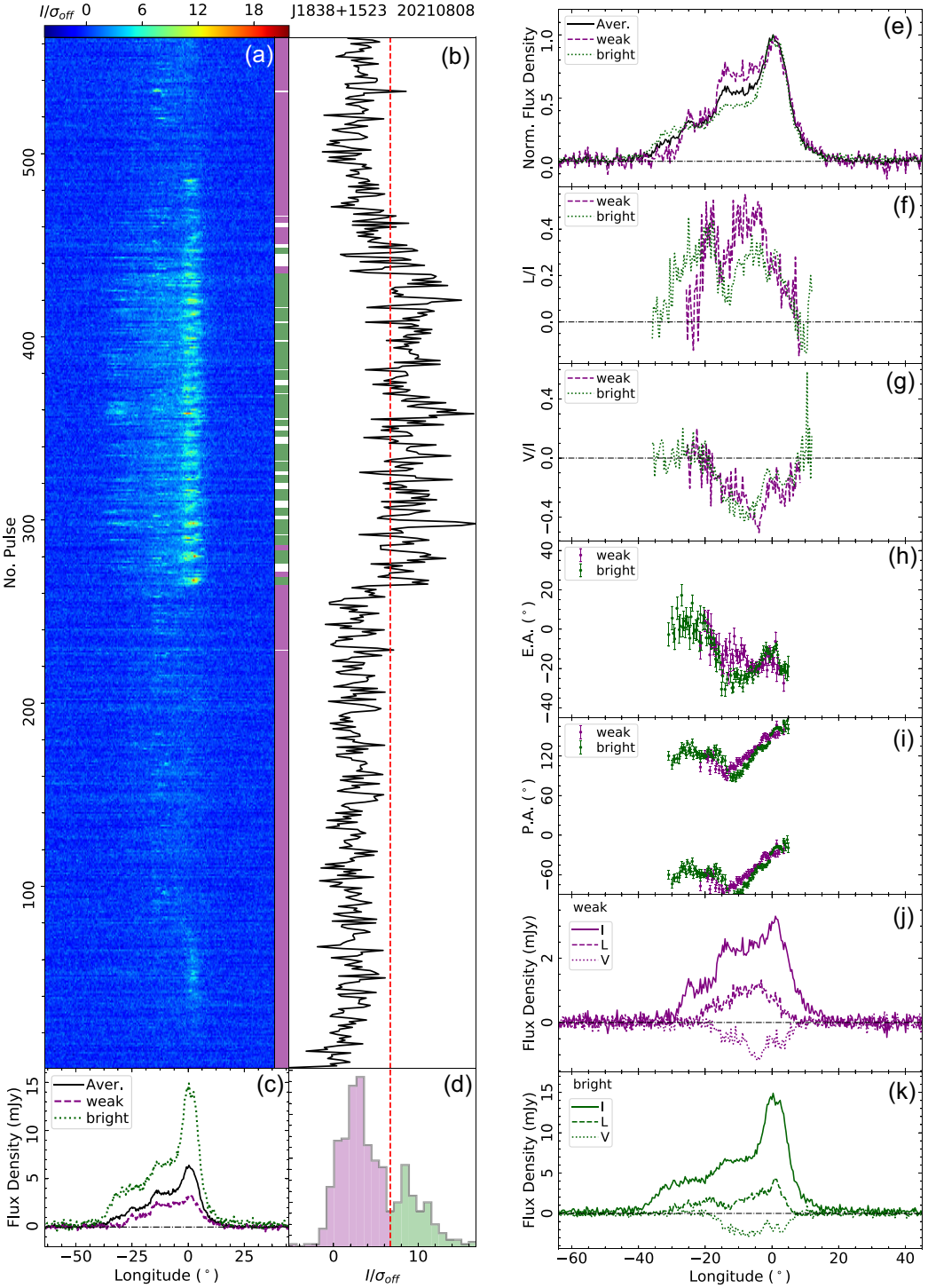

Figure 1. Individual pulses and the polarization properties for two emission states of PSR J1838+1523, observed by the FAST on 2021 August 8. The individual pulse sequence is shown in panel (a), with the variation of integrated intensity in panel (b). Bright and weak emission modes are labelled using green and purple bars along the sequence, and the pulses that cannot be discriminated are left as white. The average profiles of the two emission modes as well as all periods are shown in panel (c). The distribution of the integrated pulse intensities is shown in panel (d), which is normalized by $\sigma_{\rm off}$ obtained from the off-pulse window statistics. The two emission modes are discriminated by the threshold indicated by the vertical dashed line. Panels (e) to (k) on the right are comparisons for the total flux density pulse profiles for the weak and bright modes and all averaged periods normalized to their peak (panel e), the fractional linear polarization, *L*/*I* (panel f), the fractional circular polarization, *V*/*I* (panel g), the ellipticity angles, EA = 1/2 arctan (*V*/*L*) (panel h), the PAs of linear polarization (panel i) of the two modes, and also the averaged polarization profiles (*I*, *L*, *V*), for the weak mode (panel j) and for the bright mode (panel k). The PA and EA are plotted only when the total intensity and linear polarization intensity exceed $3\sigma_I$ and $4\sigma_L$ of the off-pulse region; *L*/*I* and *V*/*I* are plotted only when the total intensity exceeds $6\sigma_I$.

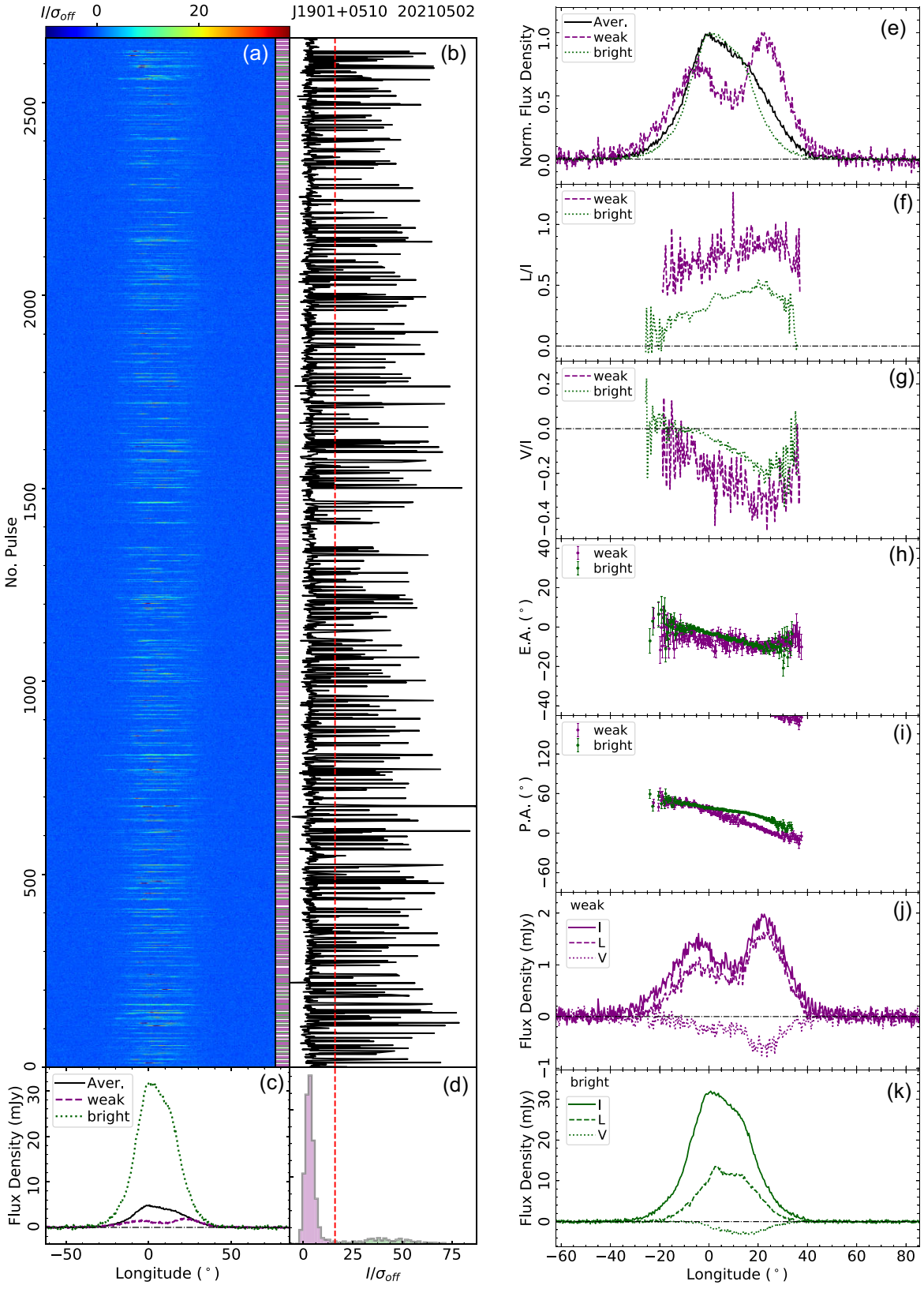

Figure 2. Same as Fig. 1 but for PSR J1901+0510 observed on 2021 May 2.

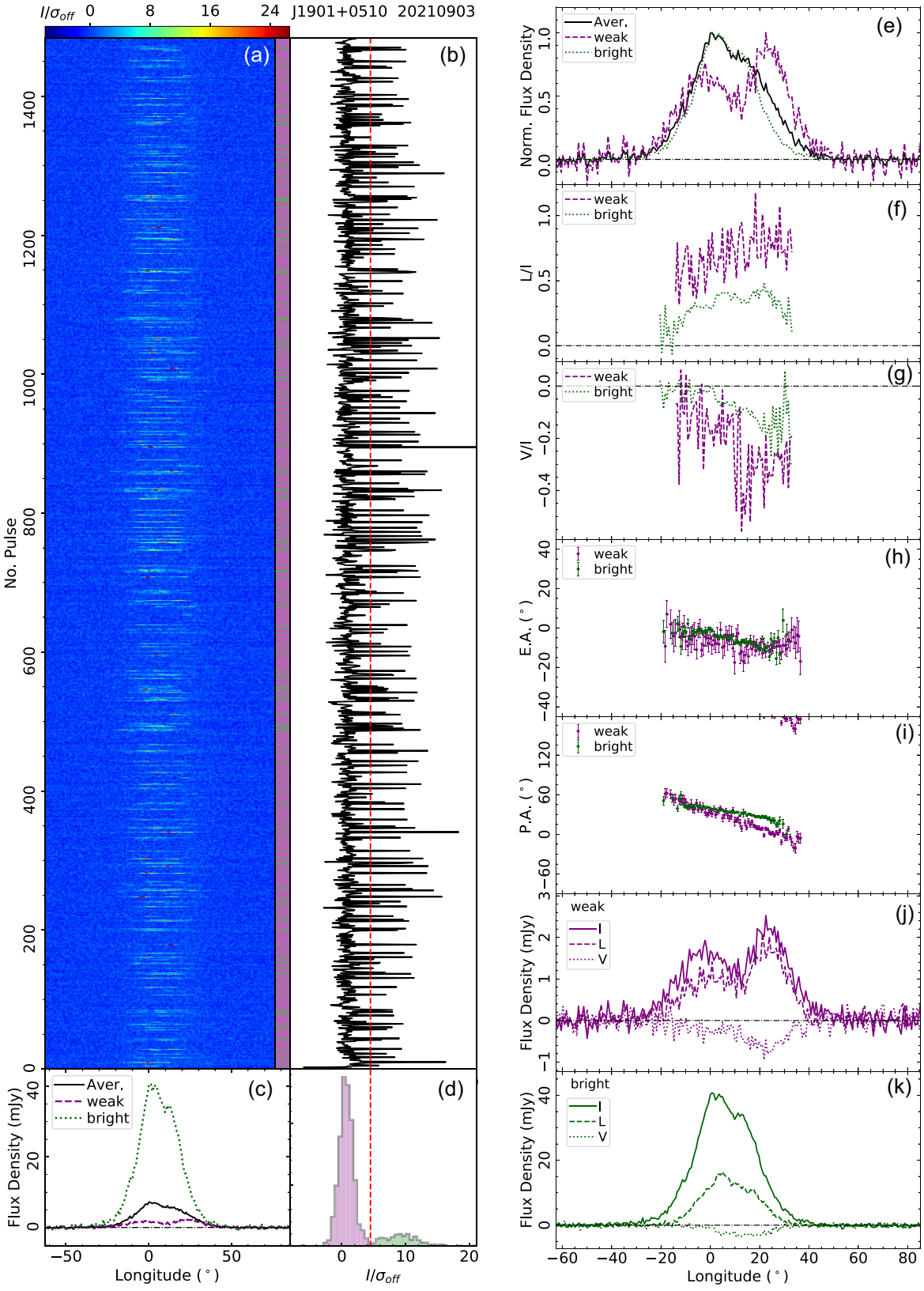

Figure 3. Same as Fig. 2 for PSR J1901+0510 but observed by FAST on 2021 September 3.

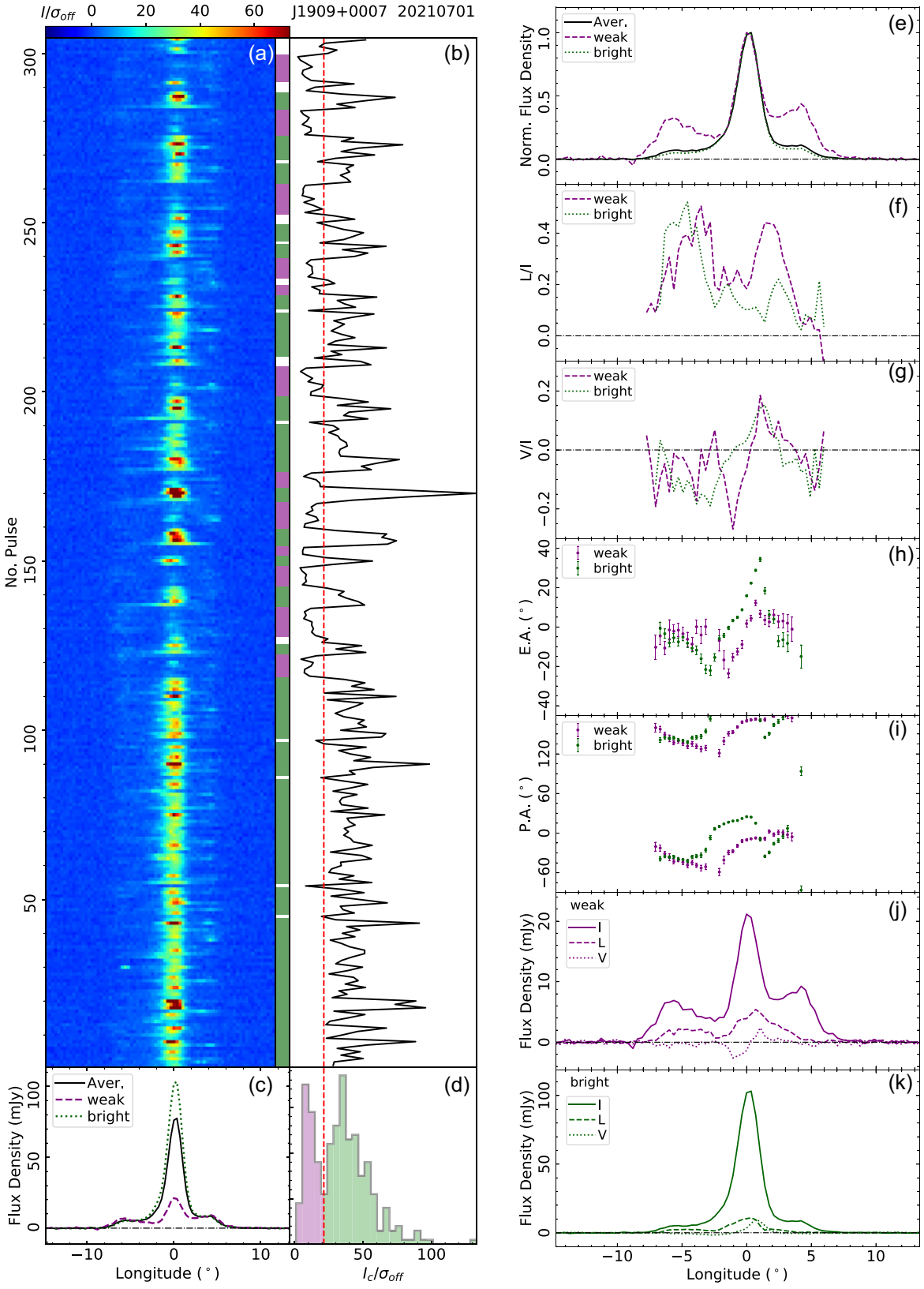

Figure 4. Same as Fig. 1 but for PSR J1909+0007 observed by FAST on 2021 July 1.

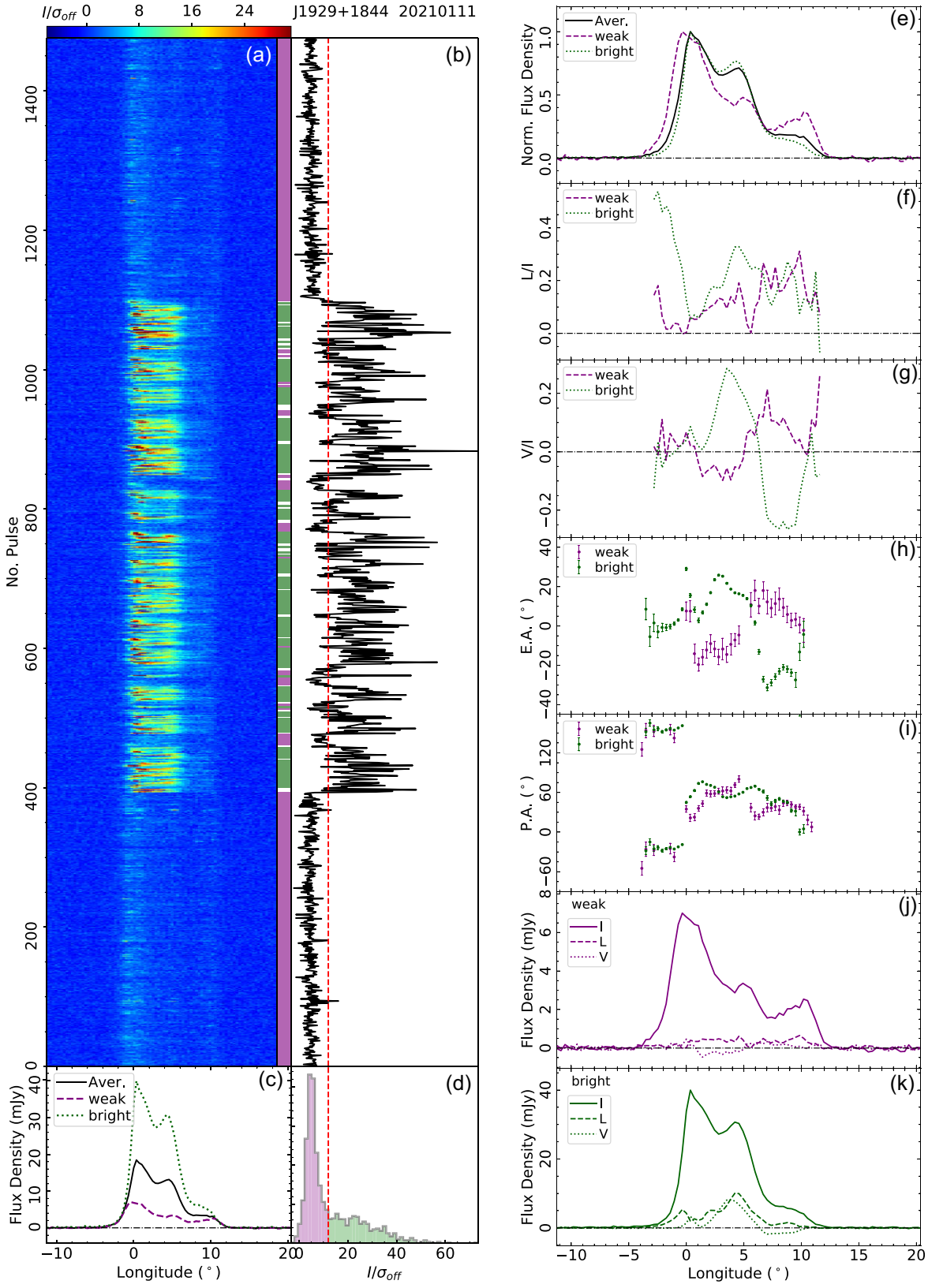

Figure 5. Same as Fig. 1 but for PSR J1929+1844 observed on 2021 January 11.

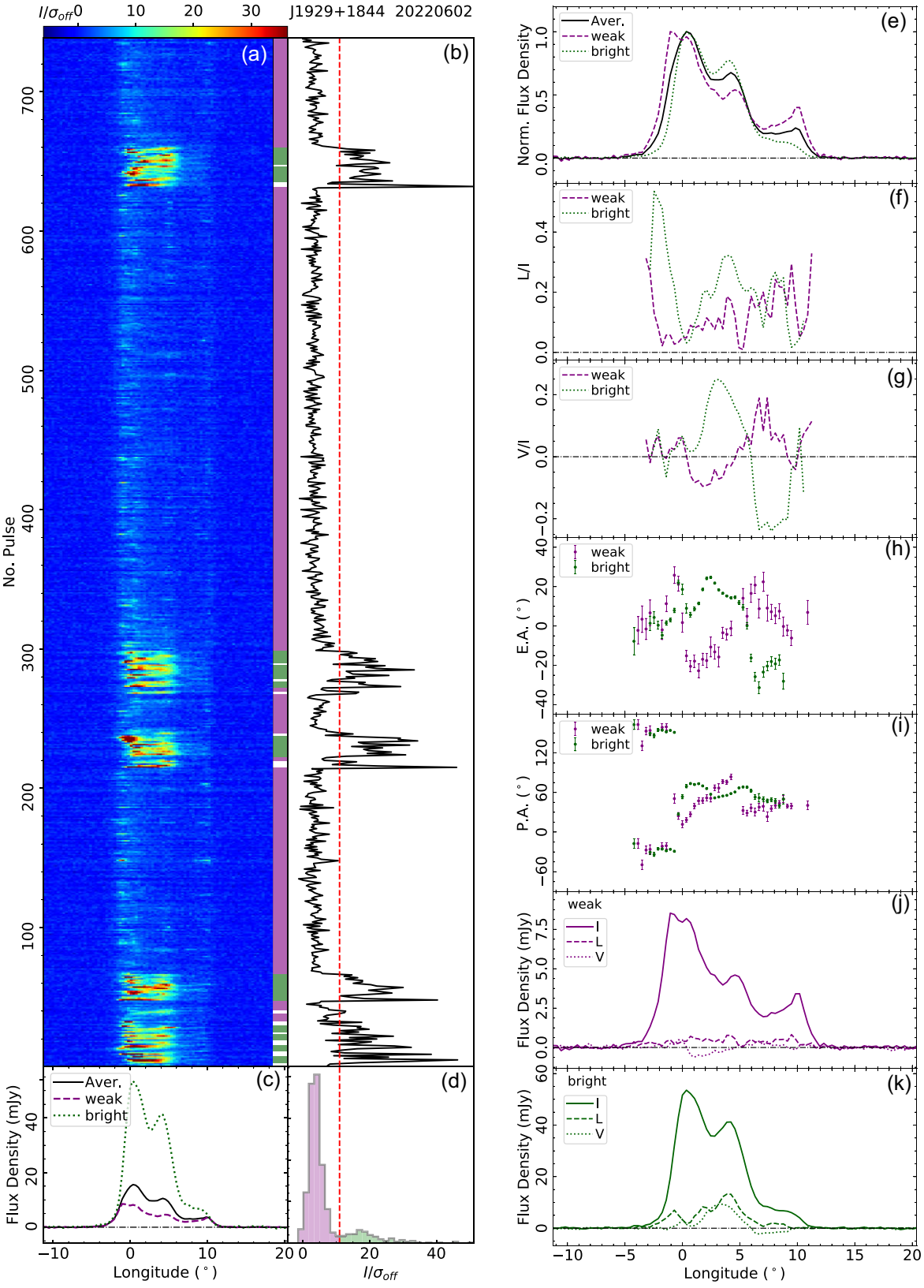

Figure 6. Same as Fig. 5 but observed on 2022 June 2.

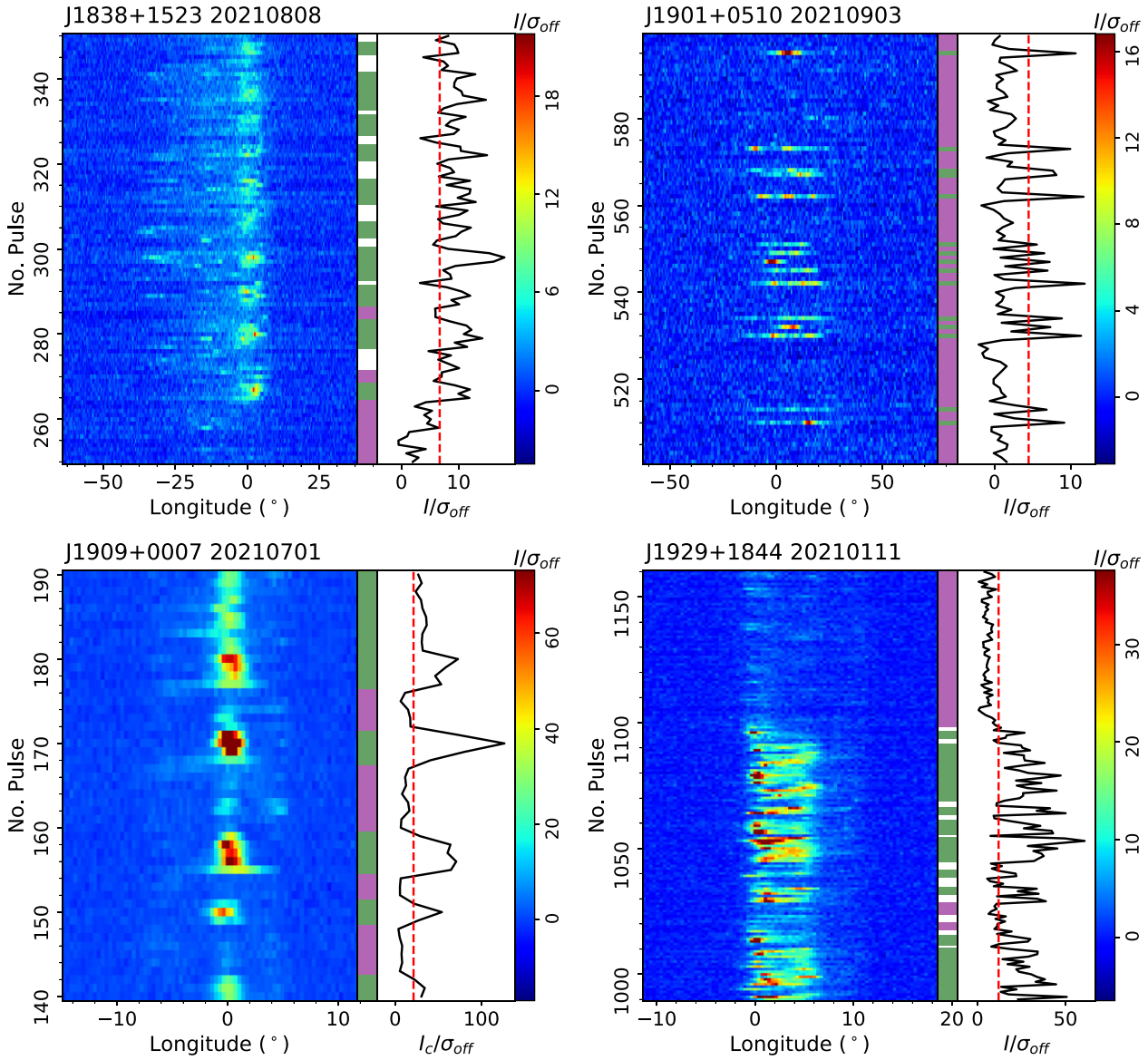

Figure 7. Zoomed-in views of some segments of pulse sequences for PSRs J1838+1523, J1901+0510, J1909+0007, and J1929+1844.

Table 2. The fractional linear and circular polarization of two emission states for four pulsars. Columns 1 and 2 give the pulsar name and the observation date. Columns 3−5 show the fractional linear, fractional absolute circular, and fractional circular polarization (*L*/*I*, |*V*|/*I*, and *V*/*I*, respectively) of the whole integrated pulse profiles. Columns 6−8 show *L*/*I*, |*V*|/*I*, and *V*/*I* of the weak emission state and Columns 9−11 show *L*/*I*, |*V*|/*I*, and *V*/*I* of the bright state. For J1909+0007, 'weak' or 'bright' are distinguished by the central component.

JName	ObsDate	Whole profile			Weak state			Bright state		
		L/*I* (%)	|*V*|/*I* (%)	*V*/*I* (%)	*L*/*I* (%)	|*V*|/*I* (%)	*V*/*I* (%)	*L*/*I* (%)	|*V*|/*I* (%)	*V*/*I* (%)
(1)	(2)	(3)	(4)	(5)	(6)	(7)	(8)	(9)	(10)	(11)
J1838+1523	2021/08/08	24.6(3)	19.2(4)	−16.8(4)	27.9(5)	22.0(8)	−20.2(8)	21.1(3)	17.0(4)	−14.4(4)
J1901+0510	2021/05/02	47.1(2)	11.9(2)	−11.4(2)	72.6(6)	22.9(7)	−21.8(7)	36.5(1)	7.5(1)	−7.1(1)
	2021/09/03	45.3(3)	11.9(5)	−11.4(5)	68.5(12)	23.3(15)	−22.2(15)	33.2(2)	7.2(2)	−6.8(2)
J1909+0007	2021/07/01	14.1(1)	6.4(1)	1.9(1)	25.1(4)	7.9(6)	−3.0(6)	13.5(1)	6.9(1)	2.7(1)
J1929+1844	2021/01/11	16.6(1)	9.0(1)	6.3(1)	9.7(3)	5.9(4)	1.2(4)	19.3(1)	12.8(1)	8.2(1)
	2022/06/02	13.6(1)	5.7(2)	4.1(2)	9.8(2)	5.2(3)	0.2(3)	18.8(1)	11.6(2)	7.9(2)

and the polarization results are consistent in the two observations. The intensity distributions exhibit two distinct groups in both Figs 2 and 3, which correspond to the bright and the weak states.

Pulsar polarization profiles for the two states are different. As shown in Figs 2 and 3, the pulse profiles on the weak state exhibit two distinct components, but the component separation of the bright state is too small to have two peaks. In addition, the polarization PA curves of the weak state on the two observation sessions have a steeper slope compared with those on the strong state, with a much larger deviation in the trailing component. The fractional linear and absolute circular polarization in the weak state is systematically higher than those for the bright state.

3.3. PSR J1909+0007

PSR J1909+0007 (B1907+00) was discovered in the low-latitude pulsar survey by the Mark 1A radio telescope at Jodrell Bank (Davies, Lyne & Seiradakis 1973).

This is the first time that the mode changing of this pulsar has been reported, based on a 5-min FAST GPPS survey observation conducted on 2021/07/01. Its leading and trailing components are occasionally brightened, whereas the central component is occasionally much weakened, as shown in Fig. 4(a). The central component exhibits two distinct distributions of intensities (see Fig. 4d), which enables the classification of single pulses into bright and weak states.

Pulsar profiles in the two states of the central component have different polarization features, as shown in the right part of Fig. 4. Intensity and polarization of the leading and trailing components remain almost unchanged during the switching of the two states, but the central component switches to the very bright state (see Fig. 4c). Effectively, the two shoulder components are enhanced in the weak mode if these profiles are scaled by the peak flux density. The polarization PAs are different by about 45°, and the fractional linear polarization is also reduced in the bright mode, both of which induce the difference of elliptic angles. These variations might be caused by the competition of the orthogonal polarization modes.

3.4. PSR J1929+1844

PSR J1929+1844 (B1926+18) was found by Arecibo at 430 MHz (Hulse & Taylor 1975). It is a canonical example of a mode-changing pulsar. The mode-changing phenomenon was previously reported by Ferguson et al. (1981). In its 'abnormal mode', all three components become bright, and the intensity of the central component is extremely enhanced (Ferguson et al. 1981; Weisberg et al. 1986; Nowakowski 1994). However, the polarization behaviours of these modes have not yet been reported previously.

We obtained two FAST observations for 30 and 15 min on 2021/01/11 and 2022/06/02, respectively, during the FAST GPPS survey verification observations for a pulsar candidate. The bright and weak states of this pulsar are clearly shown in the single pulse sequences in Figs 5 and 6. A zoomed-in view of single-pulse sequence is displayed in Fig. 7 for pulses between 990 and 1160 in Fig. 5. The bright state can last for several tens to several hundreds of periods, during which the pulsar might occasionally switch back to its normal mode. The bright and weak pulses are interspersed especially in the bright state, which leads the intensity histogram of both states to be overlapped in Figs 5(d) and 6(d).

As shown in Figs 5 and 6, the weak mode shows a wider pulse profile, and the pulse window extends from a longitude of about −3.°8 to 12.°5. There is a notch at the longitude of 0° for the weak state. When the pulsar switches to the bright state, only the pulses within the phase range of −1.°0 to 10.°5 are enhanced, which leads the notch exhibiting in the weak state to be filled. Moreover, different components are enhanced differently, with the central component growing the most and the trailing component the least. This behaviour is consistent with the previous observations at 430 MHz, although the central component is not dominating over the leading component at this FAST observation frequency.

The polarization behaviours of two emission states are remarkable. Around the pulse peak phase nearly at the longitude of 0°, the orthogonal polarization mode with a 90° jump is seen in polarization PA curves for both states. For emission prior to the peak phase, the polarization PAs remain almost consistent for the states, though the fractional linear polarization of the bright state is much higher than that of the weak state. For the emission after the peak phase, the PA curves are very different for the two states, with a possible orthogonal polarization mode jump at the longitude of 5.°0 in the weak mode. The most striking is the completely reversed senses of circular polarization for the two states, from the left hand to the right hand for the bright state, to just the opposite for the weak state. The degrees of linear and absolute circular polarization are low for the whole pulse profile in the weak mode compared with that of the bright one (see Table 2). The variation of ellipticity angles reflects both the reversals of circular polarization senses and the very different PA curves for the two states.

4. DISCUSSION

As presented above, the pulse polarization profiles, the PA curves, the fractional linear polarization, the fractional circular polarization or even the senses, can be very different for the two emission states of PSRs J1838+1523, J1901+0510, J1909+0007, and J1929+1844, which might be related to physical processes or conditions within the pulsar magnetosphere.

4.1. Different components in the two emission states

The profile components of PSR J1901+0510 vary the most during its state switching. As shown in Fig. 8, the component separation is about 15° for the bright state but widens to 28° for the weak state. Moreover, the profile centre of the weak state is delayed by approximately 1.°2 compared with that of the bright state.

Pulsar radio emission is generally believed to be generated from the open magnetic field lines of a dipole magnetosphere. Assuming that the emission of the two states is produced by the same bundle of relativistic particles, its wide profile, together with the wide component separation, suggests that the emission of the weak state originates from a larger height of the pulsar magnetosphere compared with the bright state. Moreover, according to the aberration and retardation effects, the profile originating from a higher altitude is shifted towards an earlier phase compared with emission from a lower altitude (Gangadhara & Gupta 2001). However, the profile of the weak state is delayed compared with that of the bright one. The contradiction might be caused by the asymmetry of the profile components within the pulsar conal emission beam (Xu, Qiao & Han 1997). Otherwise, the emission of the two states should originate from different bundles of relativistic particles, and the emission on the weak state is generated from a lower altitude.

In addition to the time-dependent features, the bright and weak states of the pulsar also have different frequency evolution. Fig. 9 shows profiles of the two states across four FAST observing frequency subbands from 1000 to 1500 MHz. The profiles remain almost unchanged with frequency for the weak state, while significant

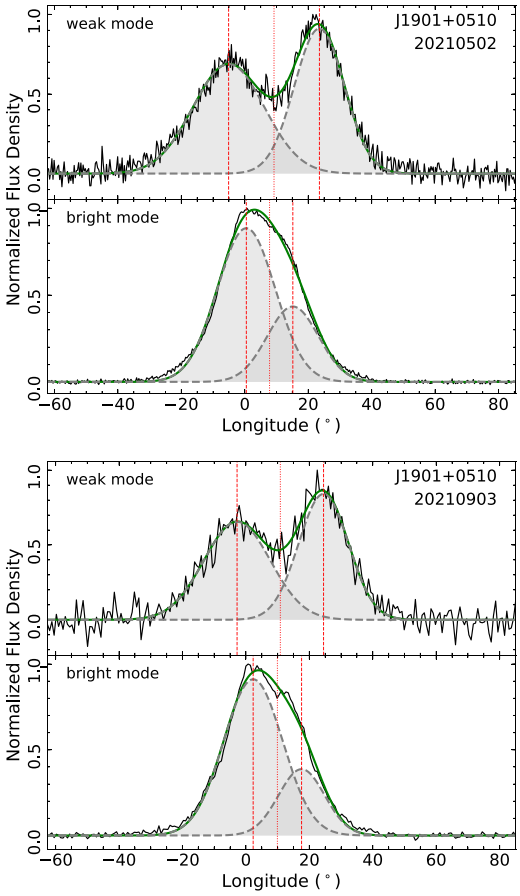

Figure 8. Component separation of the pulse profiles of PSR J1901+0510 for its two emission states observed on 2021/05/02 and 2021/09/03. The black and green solid lines are integrated pulse profiles and their fittings with a two-Gaussian function. Fitted Gaussian curves corresponding to the components are plotted using dashed grey lines. The red vertical dashed lines indicate the peak positions of the two components, and the central dotted vertical line represents the profile centre. The two components are separated by about 28° for the weak state, but only by about 15° for the bright state.

changes are observed for the bright state, mainly because the central component becomes stronger at lower frequencies and finally dominates at 430 MHz (Hulse & Taylor 1975).

4.2. Different linear polarization in the two emission states

As demonstrated in Wang & Han (2016), the fractional linear polarization can be of various degrees, depending on the interaction of the orthogonal polarization modes (X and O modes). If both modes have comparable intensities, the net fractional linear polarization will approach zero. The fraction will be high if one mode dominates over the other, as caused by rotation-induced mode separation or refraction (Wang & Han 2016).

The fractional linear polarization is very different in the two emission states of PSR J1901+0510. As listed in Table 2, it reaches about 70 per cent for emission in the weak state. As analysed in Section 4.1the emission of the weak state of PSR J1901+0510 is likely to originate from a smaller emission height, where refraction might play an important part in separating the modes, and hence the fractional linear polarization could be high.

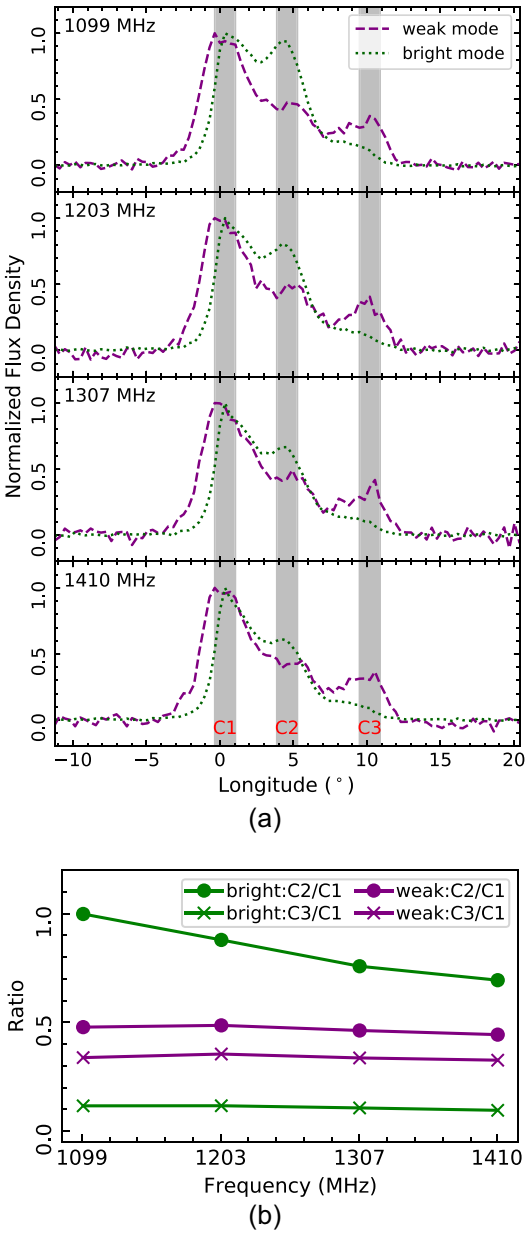

Figure 9. (a) The total intensity profiles of PSR J1929+1844 in the four subbands (1099, 1203, 1307, and 1410 MHz) of FAST observations on 2021/01/11 in the two states, and (b) the peak ratios of the main components (C1, C2, and C3) compared with the peak value of the leading peak (C1).

The strong and weak states of PSR J1909+0007 might be dominated by different polarization modes for the central component. Competition between polarization modes may be different in the two emission states, causing distinct fractional linear polarization. The main polarization mode of PSR J1929+1844 at the phase prior to the profile peak becomes more dominated when the pulsar switches to the bright state, causing a larger fractional linear polarization.

4.3. Different polarization position angle curves of the two emission states

The PAs of linear polarization exhibit different variations in the two emission states for these four pulsars. One type is the change in

the steepness of PA curves for PSRs J1838+1523 and J1901+0510, and the others include the shift of PA curves for PSR J1929+1844 and very different curves for PSR J1909+0007. These different PA curves in the two modes may have different physical origins.

The change of steepness of PA curves might be caused by the aberration effect, depending on emission heights. If the emission of the two states originates from different heights, their PA curves at the same phase have different gradients, as demonstrated in Blaskiewicz et al. (1991) and Wang, Wang & Han (2012). For example, the PA curve of PSR J1901+0510 in its weak state has a larger gradient. The slightly delayed phase of the profile centre indicates a smaller emission height for the weak mode.

The complicated shifts of PAs might result from the superposition of emission from different parts of the pulsar magnetosphere. The emission from the same region will have polarization vectors either perpendicular to or within the local magnetic field line plane. If emission originates from different parts in the magnetosphere, the magnetic field line planes are not parallel. Superposition of these will result in the variation of PAs. The central components of the bright state of PSRs J1909+0007 and J1929+1844 are likely produced in other parts of the pulsar magnetosphere compared with the weak state, as demonstrated by its distinct spectrum in Section 4.1, and the superposition of them leads to the variation of PAs.

4.4. Different circular polarization for the two emission states

The different fractional circular polarization of PSR J1901+0510 and the sense reversal of circular polarization around the central component of PSR J1929+1844 in the two emission states might be caused by different emission processes or propagation effects (e.g. Wang, Lai & Han 2010; Wang et al. 2012). Variations of density gradients of the relativistic particles will lead the fractional circular polarization to be changed, depending on the sight line (Wang et al. 2012).

5. CONCLUSIONS

In this paper, we investigate the polarization features of four pulsars that have weak and bright states. For PSRs J1838+1523, J1901+0501, and J1909+0007, this is the first time that the mode-changing features have been reported. For PSR J1929+1844, the polarization properties of both states are investigated in this paper for the first time. For these two emission states, significant differences have been observed in the profile morphology, the PAs of linear polarization, the fractions of linear and circular polarization and its senses. For PSR J1838+1523, the profile morphology, the steepness of its PA curve, and its fractional linear polarization all change between the two emission modes. For PSR J1901+0510, the profile morphology, the steepness of PA curves, and the fractional linear and circular polarization are changed for the whole pulse profile. For PSR J1909+0007, the central component exhibits very different intensity, PA, and fractional linear polarization. For PSR J1929+1844, the central component of its bright state has different frequency evolution, and exhibits significant variation of PAs, fractional linear polarization and the sense reversals of circular polarization.

These different properties of the two emission modes give insights into the physical processes and conditions of the pulsar magnetosphere. Rearrangement of the relativistic particles probably plays an important part in causing the state switchings. Its influences, aberration effect, and density gradient of relativistic particles, together with the superposition of orthogonal polarization modes, may result in various observational features during emission-state switchings.

ACKNOWLEDGEMENTS

PFW is supported by the National Key R&D Program of China (Nos 2021YFA1600401 and 2021YFA1600400), National Natural Science Foundation of China (Nos 11873058 and 12133004), and the National SKA program of China (No. 2020SKA0120200). JLH is supported by the National Natural Science Foundation of China (NSFC, Nos 11988101 and 11833009) and the Key Research Program of the Chinese Academy of Sciences (Grant No. QYZDJ-SSW-SLH021).

DATA AVAILABILITY

Original FAST observational data are open sources in the FAST Data Center according to the FAST data one-year protection policy. The folded and calibrated data in this paper can be obtained from the authors on request. All polarized pulse profile data presented in this paper are available on the webpage http://zmtt.bao.ac.cn/psr-fast/.

REFERENCES

Backer D. C., 1970, Nature, 228, 1297
Basu R., Mitra D., 2018, MNRAS, 476, 1345
Basu R., Paul A., Mitra D., 2019, MNRAS, 486, 5216
Blaskiewicz M., Cordes J. M., Wasserman I., 1991, ApJ, 370, 643
Brinkman C., Mitra D., Rankin J., 2019, MNRAS, 484, 2725
Davies J. G., Lyne A. G., Seiradakis J. H., 1973, Nat. Phys. Sci., 244, 84
Ferguson D. C., Boriakoff V., Weisberg J. M., Backus P. R., Cordes J. M., 1981, A&A, 94, L6
Gangadhara R. T., Gupta Y., 2001, ApJ, 555, 31
Geppert U., Basu R., Mitra D., Melikidze G. I., Szkudlarek M., 2021, MNRAS, 504, 5741
Han J. L. et al., 2021, Res. Astron. Astrophys., 21, 107
Hobbs G. et al., 2004, MNRAS, 352, 1439
Hotan A. W., van Straten W., Manchester R. N., 2004, PASA, 21, 302
Huguenin G. R., Taylor J. H., Troland T. H., 1970, ApJ, 162, 727
Hulse R. A., Taylor J. H., 1975, ApJ, 201, L55
Ilie C. D., Weltevrede P., Johnston S., Chen T., 2020, MNRAS, 491, 3385
Jiang P. et al., 2020, Res. Astron. Astrophys., 20, 064
Karastergiou A., Roberts S. J., Johnston S., Lee H., Weltevrede P., Kramer M., 2011, MNRAS, 415, 251
Keith M. J., Shannon R. M., Johnston S., 2013, MNRAS, 432, 3080
Lyne A., Hobbs G., Kramer M., Stairs I., Stappers B., 2010, Science, 329, 408
Manchester R. N., Hobbs G. B., Teoh A., Hobbs M., 2005, AJ, 129, 1993
Nan R., 2006, Science in China: Physics, Mechanics and Astronomy, 49, 129
Nan R. et al., 2011, Int. J. Mod. Phys. D, 20, 989
Nowakowski L. A., 1994, A&A, 281, 444
Rahaman S. K. M., Basu R., Mitra D., Melikidze G. I., 2021, MNRAS, 500, 4139
Rankin J. M., Suleymanova S. A., 2006, A&A, 453, 679
Rejep R., Wang N., Yan W. M., Wen Z. G., 2022, MNRAS, 509, 2507
Suleymanova S. A., Izvekova V. A., Rankin J. M., Rathnasree N., 1998, J. Astrophys. Astron., 19, 1
Sun S. N., Yan W. M., Wang N., Wang H. G., Wang S. Q., Dang S. J., 2022, ApJ, 934, 57
Surnis M. P., Joshi B. C., McLaughlin M. A., Lorimer D. R., M A K., Manoharan P. K., Naidu A., 2018, MNRAS, 478, 4433

Timokhin A. N., 2010, MNRAS, 408, L41
van Straten W., Bailes M., 2011, PASA, 28, 1
Wang C., Lai D., Han J., 2010, MNRAS, 403, 569
Wang N., Manchester R. N., Johnston S., 2007, MNRAS, 377, 1383
Wang P. F., Han J. L., 2016, MNRAS, 462, 4416
Wang P. F., Wang C., Han J. L., 2012, MNRAS, 423, 2464
Wang Z-W., Yuan M., Wang L., Zhang C-M., Peng B., 2022, Res. Astron. Astrophys., 22, 075002
Weisberg J. M., Armstrong B. K., Backus P. R., Cordes J. M., Boriakoff V., Ferguson D. C., 1986, AJ, 92, 621
Xu R. X., Qiao G. J., Han J. L., 1997, A&A, 323, 395

This paper has been typeset from a TEX/LATEX file prepared by the author.